Electronic Supplementary Information

Parahydrogen Allows Ultra-Sensitive Indirect NMR Detection of Catalytic Hydrogen Complexes

Alexey S. Kiryutin,[1,2] Grit Sauer,[3] Alexandra V. Yurkovskaya[1,2], Hans-Heinrich Limbach,[4] Konstantin L. Ivanov,[1,2*] Gerd Buntkowsky[3*]

[1]*International Tomography Center, Institutskaya 3A, Novosibirsk, 630090, Russia.*

[2]*Novosibirsk State University, Pirogova 2, Novosibirsk, 630090, Russia*

[3]*Technische Universität Darmstadt, Eduard-Zintl-Institut für Anorganische und Physikalische Chemie, Alarich-Weiss-Straße 8, Darmstadt, 64287, Germany*

[4] *Freie Universität Berlin, Institut für Chemie und Biochemie, Takustraße 3, Berlin, 14195, Germany*

Quantitative Analysis of the PNL employing Liouville Space Formalism

The equations of motion for the density matrix in Liouville space are ($|\hat{\rho}_a)$: free dissolved H_2; $|\hat{\rho}_b)$: M-H_2 complex):

$$\frac{d}{dt}|\hat{\rho}_a) = -i\hat{\hat{L}}_a|\hat{\rho}_a) - k_f|\hat{\rho}_a) + k_d|\hat{\rho}_b) \tag{1}$$

$$\frac{d}{dt}|\hat{\rho}_b) = -i\hat{\hat{L}}_b|\hat{\rho}_b) - k_d|\hat{\rho}_b) + k_f|\hat{\rho}_a)$$

Here, $\hat{\hat{L}}_a$ and $\hat{\hat{L}}_b$ are the Liouville operators of the corresponding species. For $|\hat{\rho}_b)$ we can assume a quasi-stationary state:

$$\frac{d}{dt}|\hat{\rho}_b) = -i\hat{\hat{L}}_b|\hat{\rho}_b) - k_d|\hat{\rho}_b) + k_f|\hat{\rho}_a) \approx 0 \tag{2}$$

Solving for $|\hat{\rho}_b)$ gives:

$$\begin{aligned} \left(k_d + i\hat{\hat{L}}_b\right)|\hat{\rho}_b) &= k_f|\hat{\rho}_a) \\ |\hat{\rho}_b) &= k_f\left(k_d + i\hat{\hat{L}}_b\right)^{-1}|\hat{\rho}_a) \end{aligned} \tag{3}$$

In the general cases of strong or intermediate coupling $\hat{\hat{L}}_b$ will be non-diagonal and the inversion of $\left(k_d + i\hat{\hat{L}}_b\right)$ is feasible only numerically. However, in the case of weak coupling ($|\nu_I - \nu_S| >> J_{IS}$) the Liouvillian $\hat{\hat{L}}_b$ is diagonal

$$\left(k_d + i\hat{\hat{L}}_b\right)_{mm} = k_d + i\hat{\hat{L}}_{b,mm}\ , \tag{4}$$

allowing for an analytic calculation of the PNL, which gives more physical insights than the numeric solution. Since already for shift-differences of 1 ppm the weak coupling condition will be at least approximately fulfilled for most dihydrides, this is also not a too severe limitation. In this case it is easy to invert the matrix:

$$k_f\left(\left(k_d + i\hat{\hat{L}}_b\right)^{-1}\right)_{mm} = \frac{k_f}{k_d + iL_{b,mm}} = \frac{k_f k_d}{{k_d}^2 + {L_{b,mm}}^2} - i\frac{k_f L_{b,mm}}{{k_d}^2 + {L_{b,mm}}^2} \tag{5}$$

As shortcut we define two new diagonal super-operators $\hat{\hat{A}}_R$ and $\hat{\hat{A}}_I$, whose elements are

$$A_{R,mm} = \left(\frac{k_f k_d}{{k_d}^2 + {L_{b,mm}}^2} \right) \text{ and } \quad A_{I,mm} = -\frac{k_f L_{b,mm}}{{k_d}^2 + {L_{b,mm}}^2} \ , \tag{6}$$

leading to

$$\left|\hat{\rho}_b\right) = \left(\hat{\hat{A}}_R + i\hat{\hat{A}}_I \right) \left|\hat{\rho}_a\right) \ . \tag{7}$$

Inserting into in the equation for $\left|\hat{\rho}_a\right)$ gives

$$\begin{aligned} \frac{d}{dt}\left|\hat{\rho}_a\right) &= -i\hat{\hat{L}}_a \left|\hat{\rho}_a\right) - k_f \left|\hat{\rho}_a\right) + k_d \left(\hat{\hat{A}}_R + i\hat{\hat{A}}_I \right) \left|\hat{\rho}_a\right) \\ &= -\left(k_f - k_d \hat{\hat{A}}_R \right) \left|\hat{\rho}_a\right) - i\left(\hat{\hat{L}}_a - k_d \hat{\hat{A}}_I \right) \left|\hat{\rho}_a\right) = -\left(\hat{\hat{K}}_{eff} + i\hat{\hat{L}}_{eff} \right) \left|\hat{\rho}_a\right) \end{aligned} \tag{8}$$

with $\hat{\hat{K}}_{eff} = \left(k_f - k_d \hat{\hat{A}}_R \right)$ and $\hat{\hat{L}}_{eff} = \left(\hat{\hat{L}}_a - k_d \hat{\hat{A}}_I \right) = \hat{\hat{L}}_a - \hat{\hat{L}}_M$.

In the case of weak coupling $\hat{\hat{K}}_{eff}$ is diagonal in the Zeeman basis

$$K_{eff,mm} = k_f - k_d \left(\frac{k_f k_d}{{k_d}^2 + {L_{b,mm}}^2} \right) = \frac{k_f {L_{b,mm}}^2}{{k_d}^2 + {L_{b,mm}}^2} \tag{9}$$

The same is true for the correction term $\hat{\hat{L}}_M$:

$$L_{M,mm} = k_d A_{I,mm} = -\frac{k_f k_d L_{b,mm}}{{k_d}^2 + {L_{b,mm}}^2} \ . \tag{10}$$

To calculate the changes of the frequencies by perturbation theory we transform $\hat{\hat{L}}_M$ into the singlet-triplet base:

$$\hat{\hat{L}}_{Mst} = R_{st} \hat{\hat{L}}_M R_{st}^{-1} \tag{11}$$

The transformation super-operator is calculated as direct product from the Hilbert-space operator as

$$R_{st} = \begin{pmatrix} 1 & 0 & 0 & 0 \\ 0 & 1/\sqrt{2} & 1/\sqrt{2} & 0 \\ 0 & 1/\sqrt{2} & -1/\sqrt{2} & 0 \\ 0 & 0 & 0 & 1 \end{pmatrix} \otimes \begin{pmatrix} 1 & 0 & 0 & 0 \\ 0 & 1/\sqrt{2} & 1/\sqrt{2} & 0 \\ 0 & 1/\sqrt{2} & -1/\sqrt{2} & 0 \\ 0 & 0 & 0 & 1 \end{pmatrix} \tag{12}$$

In first order perturbation theory the shifts are given by the diagonal-elements of L_{Mst} :

$$\Delta\omega_{mm} = \left(\hat{\hat{L}}_{Mst}\right)_{mm} \tag{13}$$

To see, which frequencies are relevant, we examine the detection operator transformed to a Liouville vector. In the singlet-triplet basis we have

$$\left(\hat{F}_{+}\right| = \left(\hat{I}_{+} + \hat{S}_{+}\right| = \left(0,\sqrt{2},0,0,0,0,\sqrt{2},0,0,0,0,0,0,0,0\right| \tag{14}$$

Thus only element 2 and element 7 contribute to the FID.

$$\Delta\omega_{22} = \left(\hat{\hat{L}}_{Mst}\right)_{22} = -\frac{1}{2}\frac{k_f k_d \omega_{12}}{k_d{}^2 + \omega_{12}{}^2} - \frac{1}{2}\frac{k_f k_d \omega_{13}}{k_d{}^2 + \omega_{13}{}^2} \tag{15}$$

$$\Delta\omega_{77} = \left(\hat{\hat{L}}_{Mst}\right)_{77} = -\frac{1}{2}\frac{k_f k_d \omega_{24}}{k_d{}^2 + \omega_{24}{}^2} - \frac{1}{2}\frac{k_f k_d \omega_{34}}{k_d{}^2 + \omega_{34}{}^2} \tag{16}$$

In the case of **weak coupling** ($|\nu_I - \nu_S| >> J_{IS}$) the transition frequencies relative to the frequency of free hydrogen are given as

$$\begin{aligned}
\omega_{12} &= \left(\omega_I - \omega_H + \pi J_{IS}\right) \\
\omega_{13} &= \left(\omega_S - \omega_H + \pi J_{IS}\right) \\
\omega_{24} &= \left(\omega_I - \omega_H - \pi J_{IS}\right) \\
\omega_{34} &= \left(\omega_S - \omega_H - \pi J_{IS}\right).
\end{aligned} \tag{17}$$

Inserting these values and the equilibrium constant

$$K_{eq} = \frac{k_f}{k_d} \tag{18}$$

gives

$$\Delta\omega_{22} = -\frac{1}{2}\frac{K_{eq} k_d{}^2 \left(\omega_I - \omega_H + \pi J_{IS}\right)}{k_d{}^2 + \left(\omega_I - \omega_H + \pi J_{IS}\right)^2} - \frac{1}{2}\frac{K_{eq} k_d{}^2 \left(\omega_S - \omega_H + \pi J_{IS}\right)}{k_d{}^2 + \left(\omega_S - \omega_H + \pi J_{IS}\right)^2} \tag{19}$$

$$\Delta\omega_{77} = -\frac{1}{2}\frac{K_{eq} k_d{}^2 \left(\omega_I - \omega_H - \pi J_{IS}\right)}{k_d{}^2 + \left(\omega_I - \omega_H - \pi J_{IS}\right)^2} - \frac{1}{2}\frac{K_{eq} k_d{}^2 \left(\omega_S - \omega_H - \pi J_{IS}\right)}{k_d{}^2 + \left(\omega_S - \omega_H - \pi J_{IS}\right)^2} \tag{20}$$

The corresponding shifted resonance frequencies of the H_2 line are:

$$\omega_{1,2} = \omega_H - \frac{1}{2}\frac{K_{eq}k_d{}^2\left(\omega_I - \omega_H \pm \pi J_{IS}\right)}{k_d{}^2 + \left(\omega_I - \omega_H \pm \pi J_{IS}\right)^2} - \frac{1}{2}\frac{K_{eq}k_d{}^2\left(\omega_S - \omega_H \pm \pi J_{IS}\right)}{k_d{}^2 + \left(\omega_S - \omega_H \pm \pi J_{IS}\right)^2} \quad (21)$$

The difference between these two lines is

$$\Delta\omega = \omega_2 - \omega_1 = \frac{K_{eq}k_d{}^2}{2} \times\left(\frac{\left(\omega_I - \omega_H + \pi J_{IS}\right)}{k_d{}^2 + \left(\omega_I - \omega_H + \pi J_{IS}\right)^2} - \frac{\left(\omega_I - \omega_H - \pi J_{IS}\right)}{k_d{}^2 + \left(\omega_I - \omega_H - \pi J_{IS}\right)^2} + \frac{\left(\omega_S - \omega_H + \pi J_{IS}\right)}{k_d{}^2 + \left(\omega_S - \omega_H + \pi J_{IS}\right)^2} - \frac{\left(\omega_S - \omega_H - \pi J_{IS}\right)}{k_d{}^2 + \left(\omega_S - \omega_H - \pi J_{IS}\right)^2}\right) \quad (22)$$

For small values of J_{IS}, we can expand this expression as

$$\Delta\omega \approx \frac{K_{eq}k_d{}^2}{2} 2\pi J_{IS}\left(\frac{k_d{}^2 - \left(\omega_I - \omega_H\right)^2}{\left(k_d{}^2 + \left(\omega_I - \omega_H\right)^2\right)^2} + \frac{k_d{}^2 - \left(\omega_S - \omega_H\right)^2}{\left(k_d{}^2 + \left(\omega_S - \omega_H\right)^2\right)^2}\right) \quad (23)$$

This expression shows that the relative phase of the two lines is given by the sign of J_{IS} and the line-shape can thus be employed to determine this sign. Dividing by 2π gives the frequency difference of the two lines:

$$\Delta\nu \approx \frac{K_{eq}k_d{}^2}{2} J_{IS}\left(\frac{k_d{}^2 - \left(\omega_I - \omega_H\right)^2}{\left(k_d{}^2 + \left(\omega_I - \omega_H\right)^2\right)^2} + \frac{k_d{}^2 - \left(\omega_S - \omega_H\right)^2}{\left(k_d{}^2 + \left(\omega_S - \omega_H\right)^2\right)^2}\right) \quad (24)$$

Thus the frequency difference of the two lines of the H_2 signal is **proportional to the J_{IS}-coupling in the L_nMH_2 complex times the equilibrium constant**.

Calculations with 500 MHz spectrometer frequency and J_{IS}=100Hz gives a typical frequency difference of ca 0.04Hz with K_{eq}=0.01.

Calculation of amplitudes of the PNL:

The initial density matrix in the ST-base of the Liouville space is

$$\left|\hat{\rho}_0\right) = \left|\mathrm{p}_+,0,0,0,0,\mathrm{p}_0,0,0,0,0,\mathrm{p}_-,0,0,0,0,\mathrm{p}_\mathrm{s}\right), \tag{25}$$

where $\mathrm{p}_+,\mathrm{p}_0,\mathrm{p}_-,\mathrm{p}_\mathrm{s}$ are the initial populations of the three triplet-states $\left(\left|\left|T_+\right\rangle\right\rangle,\left|\left|T_0\right\rangle\right\rangle,\left|\left|T_-\right\rangle\right\rangle\right)$ and the singlet state $\left(\left|S\right\rangle\right)$.

The pulse super-operator is

$$\hat{\hat{P}}_{y,\varphi} = \exp\left(-i\varphi\left(\hat{\hat{I}}_y + \hat{\hat{S}}_y\right)\right) = \exp\left(-i\varphi\hat{\hat{F}}_y\right) \tag{26}$$

The density vector after the pulse is

$$\left|\hat{\rho}_{+0}\right) = \hat{\hat{P}}_{y,\varphi}\left|\hat{\rho}_0\right) = \exp\left(-i\varphi\hat{\hat{F}}_y\right)\left|\hat{\rho}_0\right) \tag{27}$$

For the calculation of the signal we need only the 2 and 7 elements:

$$\left|\hat{\rho}_{+0}\right)_2 = \frac{1}{2\sqrt{2}}\sin(\varphi)\left(1-\cos(\varphi)\right)p_- + \frac{1}{\sqrt{2}}\sin(\varphi)\cos(\varphi)\,p_0 - \frac{1}{2\sqrt{2}}\sin(\varphi)\left(1+\cos(\varphi)\right)p_+ \tag{28}$$

$$\left|\hat{\rho}_{+0}\right)_7 = \frac{1}{2\sqrt{2}}\sin(\varphi)\left(1+\cos(\varphi)\right)p_- - \frac{1}{\sqrt{2}}\sin(\varphi)\cos(\varphi)\,p_0 - \frac{1}{2\sqrt{2}}\sin(\varphi)\left(1-\cos(\varphi)\right)p_+ \tag{29}$$

The amplitudes of the lines are obtained by multiplying with the corresponding elements of $\left(\hat{F}_+\right| = \left(\hat{I}_+ + \hat{S}_+\right|$.

The first line has the amplitude (as a function of pulse angle):

$$A_1 = \frac{1}{2}\sin(\varphi)\left(1-\cos(\varphi)\right)p_- + \sin(\varphi)\cos(\varphi)\,p_0 - \frac{1}{2}\sin(\varphi)\left(1+\cos(\varphi)\right)p_+ \tag{30}$$

The second line has the amplitude (as a function of pulse angle):

$$A_2 = \frac{1}{2}\sin(\varphi)\left(1+\cos(\varphi)\right)p_- - \sin(\varphi)\cos(\varphi)\,p_0 - \frac{1}{2}\sin(\varphi)\left(1-\cos(\varphi)\right)p_+ \tag{31}$$

We can rewrite these expressions by collecting the single-spin and two-spin terms as:

$$A_1 = \frac{p_- - p_+}{2}\sin(\varphi) + \frac{2p_0 - (p_+ + p_-)}{4}\sin(2\varphi) \tag{32}$$

and

$$A_2 = \frac{p_- - p_+}{2}\sin(\varphi) - \frac{2p_0 - (p_+ + p_-)}{4}\sin(2\varphi) \tag{33}$$

In the special case that the $|T_+\rangle$ and $|T_-\rangle$ sublevels are empty and a 45° pulse is applied, the amplitudes of the PNL are

$$A_1\left(\frac{\pi}{4}\right) = \frac{p_0}{2} \tag{34}$$

and

$$A_2\left(\frac{\pi}{4}\right) = -\frac{p_0}{2} = -A_1\left(\frac{\pi}{4}\right) \tag{35}$$

Size of the PNL, compared to its components:

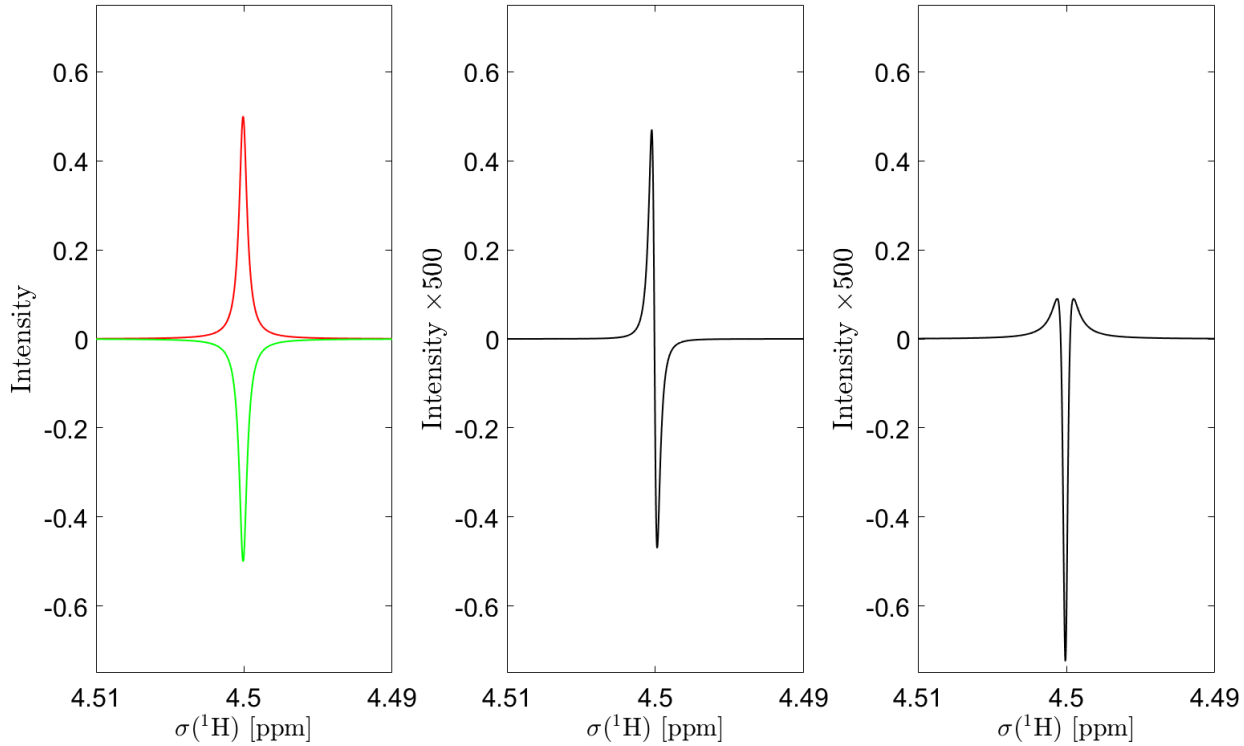

Figure S1. Calculated amplitudes of the PNL. Left: line 1 (red) and line 2 (green) forming the PNL; center: real part of PNL, which is the sum of the two lines shown in the left panel; right: imaginary part of PNL.

Analysis of the PANEL Experiment for the Detection of transient Intermediates employing Liouville Space Formalism

In the following a simple derivation of the PArtially NEgative Line (PANEL) experiment in the cw limit is given. The PANEL experiment irradiates a long narrow-band radio frequency (RF) pulse with amplitude ω_1, whose frequency ω_{CW} is swept through the spectrum.

The free hydrogen state (a) and the bound hydrogen state (b) are described by their individual spin Hamiltonians:

$$\hat{H}_a = -(\omega_{HH} - \omega_{CW})\left(\hat{S}_z + \hat{I}_z\right) + \omega_1\left(\hat{S}_x + \hat{I}_x\right) + 2\pi J_{HH}\left(\hat{S}_x\hat{I}_x + \hat{S}_y\hat{I}_y + \hat{S}_z\hat{I}_z\right) \tag{36}$$

and

$$\hat{H}_b = -(\omega_S - \omega_{CW})\hat{S}_z - (\omega_S - \omega_{CW})\hat{I}_z + \omega_1\left(\hat{S}_x + \hat{I}_x\right) + 2\pi J_{IS}\left(\hat{S}_x\hat{I}_x + \hat{S}_y\hat{I}_y + \hat{S}_z\hat{I}_z\right) \tag{37}$$

From these Hamiltonian we can set up the equations of motions of the density operators of the free $\hat{\rho}_a$ and bound $\hat{\rho}_b$ hydrogen in Liouville space:

$$\frac{d}{dt}\left|\hat{\rho}_a\right) = -\left(\hat{\hat{R}}_a + i\hat{\hat{L}}_a\right)\left|\hat{\rho}_a\right) - k_f\left|\hat{\rho}_a\right) + k_d\left|\hat{\rho}_b\right) \tag{38}$$

$$\frac{d}{dt}\left|\hat{\rho}_b\right) = -\left(\hat{\hat{R}}_b + i\hat{\hat{L}}_b\right)\left|\hat{\rho}_b\right) - k_d\left|\hat{\rho}_b\right) + k_f\left|\hat{\rho}_a\right) \tag{39}$$

Here $\hat{\hat{L}}_n = \hat{H}_n \otimes \hat{E}_n - \hat{E}_n \otimes \hat{H}_n$ are the Liouville and $\hat{\hat{R}}_n$ the relaxation superoperators ($n = a,b$) of the free and bound hydrogen and k_f and k_d are the formation and dissociation rate of the bound hydrogen.

These two equations can be combined into a single equation in composite Liouville space,

$$\frac{d}{dt}\left|\hat{\rho}\right) = -\hat{\hat{M}}\left|\hat{\rho}\right) + \frac{1}{T_{eq}}\left|\hat{\rho}_0\right) \tag{40}$$

where $\hat{\hat{M}} = \left(\hat{\hat{R}}_a + i\hat{\hat{L}}_a\right) \oplus \left(\hat{\hat{R}}_b + i\hat{\hat{L}}_b\right)$ is a superoperator describing the dynamics in the composite Liouville space, $\left|\hat{\rho}_0\right)$ is the steady state of the system and T_{eq} is the time constant, with which the steady state is approached. For long pulses an effective equilibrium is established as

$$\frac{d}{dt}\left|\hat{\rho}_{eq}\right) \approx 0 = -\hat{\hat{M}}\left|\hat{\rho}_{eq}\right) + \frac{1}{T_{eq}}\left|\hat{\rho}_0\right) \tag{41}$$

Solving this linear equation for the equilibrium density matrix gives

$$\left|\hat{\rho}_{eq}\right) = \hat{\hat{M}}^{-1}\frac{1}{T_{eq}}\left|\hat{\rho}_{0}\right) \tag{42}$$

In the case of the PNL the NMR signal $A_{PNL}\left(\omega_{CW},\omega_1\right)$ is given as

$$A_{PNL}\left(\omega_{CW},\omega_1\right) = \frac{1}{4}\left(2\hat{T}_0 - \hat{T}_+ - \hat{T}_-\left|\hat{\rho}_{eq}\right.\right) \tag{43}$$

and in the case of z-magnetization the NMR signal $A_Z\left(\omega_{CW},\omega_1\right)$ is given as

$$A_Z\left(\omega_{CW},\omega_1\right) = \frac{1}{2}\left(\hat{S}_z + \hat{I}_z\left|\hat{\rho}_{eq}\right.\right). \tag{44}$$

The steady state density matrix $\left|\hat{\rho}_{0,PNL}\right)$ for the PANEL experiment is given as (ε_p is the enrichment factor of parahydrogen).

$$\left|\hat{\rho}_{0,PNL}\right) = \varepsilon_p\left|S\right) \tag{45}$$

For *p*-H_2 freshly prepared at liquid nitrogen temperature (77 K) $\varepsilon_p \approx 0.5$.

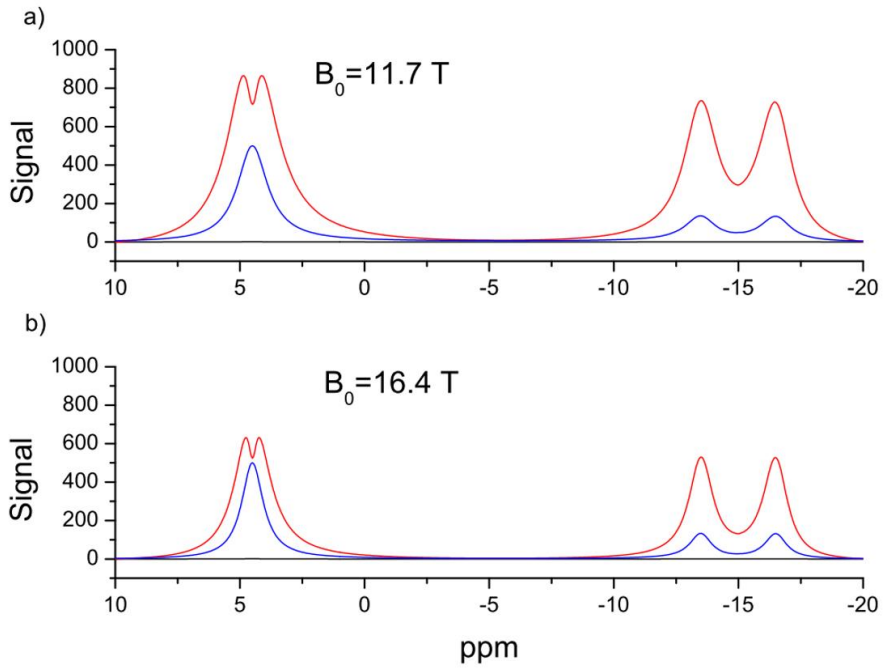

Figure S2. Comparison of the calculated signals of the PANEL experiment (red line), shown in absorption mode, relative to thermal polarization (black line) and thermal polarization multiplied by 500 (blue line) for an 11.7 T and a 16.4 T spectrometer as a function of the position of the RF irradiation in ppm. Parameters: k_f=1 sec^{-1}, k_d=1000 sec^{-1}, J_{IS}=100 Hz. T_1=T_2=1 sec^{-1}, δ_I=-13.5 ppm, δ_S=-16.5 ppm, δ_{H2}= 4.5 ppm, $\omega_1/2\pi = 260\text{Hz}$.

The steady state density matrix for the NMR experiment at thermal equilibrium is given as

$$\left|\hat{\rho}_{0,Z}\right) = \varepsilon_Z \left|\hat{S}_z + \hat{I}_z\right) , \tag{46}$$

with $\varepsilon_Z = \gamma B_0 / k_B T$. For NMR spectrometers of 500 MHz to 700 MHz at room temperature this corresponds to values of $\varepsilon_Z \approx (8 \ldots 11) \times 10^{-5} \approx 10^{-4}$.

The sensitive enhancement of the PNL versus the direct detection of the thermal NMR signal is then proportional to the ratio:

$$\lambda = \frac{\varepsilon_p}{\varepsilon_Z} , \tag{47}$$

Selective pulse excitation experiment

Figure S3 shows two PNL spectra detected with narrow bandwidth selective pulse excitation after bubbling the catalyst solution by parahydrogen, employing the "Eburp2" sequence.[1] Duration of shaped pulse was 6 ms, RF power was adjusted to have 45° or 135° flip angle. The center of excitation was set to 4.5 ppm, approximate excitation bandwidth is about 2 ppm. The band-width of the selective pulse is chosen in such a way that it excites only the region of dissolved H_2 and does not affect the signal of intermediate complexes. This key experiment proves that the partially negative line is formed after the detection pulse during the free induction decay and the initial order comes from the overpopulated T_0 state of *o*-H_2 (second pathway Scheme 4 in the main text).

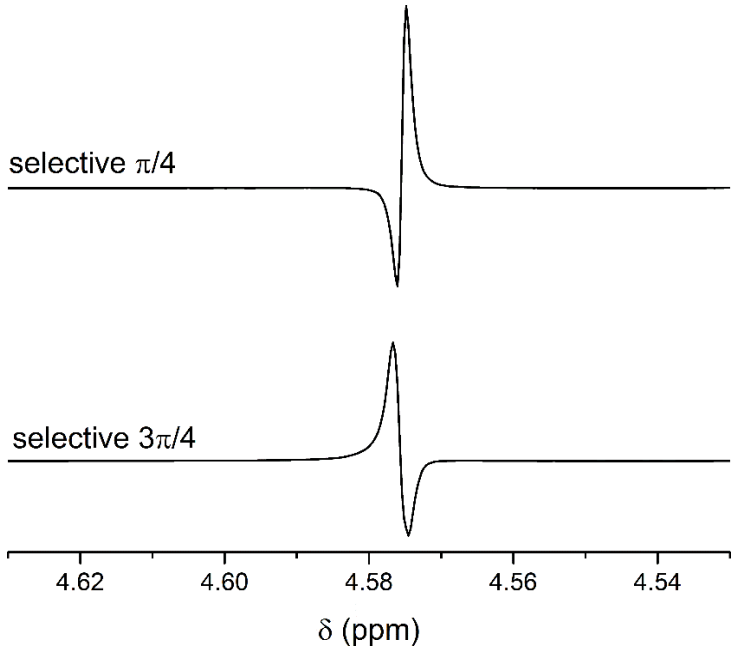

Figure S3. ^{1}H 500 MHz NMR spectra catalyst solution (3.3 mM) in acetone-d_6 taken 2 seconds after bubbling by p-H_2 using selective pulse excitation with 45° (upper panel) and 135° (lower panel).

Activation and degradation study of the catalyst in acetone-d_6

In the following section the activation and degradation of the catalyst in acetone-d_6 due to hydrogenation of cyclooctadiene (COD) is shown. Three consecutive experimets were performed. For each experiment the solution of 2.5 mg cat (Figure S4) in 600 µl acetone-d_6 was bubbled with parahydrogen for 20 s and a time depended spectra series was recored with 5 degree detection pulses. Subsequently, a thermal spectrum of the hydride region was accumulated with 512 scans during 30 min under a hydrogen pressure of 3 bar.

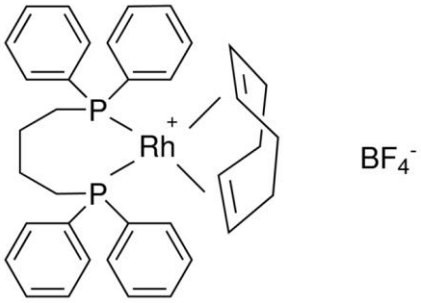

Figure S4. Structure of catalyst [1,4-bis(diphenylphosphino)butane](1,5-cyclooctadiene)rhodium(I) tetrafluoroborate

In the first bubbling period (Figure S5) the activation of the catalyst can be observed. In a first hydrogenation step the bound cyclooctadiene (COD) ligand is hydrogenated to cyclooctene (COE), COE leaves the catalyst and the active species of the solvated complex is formed.In a second hydrogenation, COE can be hydrogenated to cycloctane (COA). In the spectrum B the hyperpolarized signal of free COE around 1.5 ppm is visble. Additionally the PNL is observable at 4.55 ppm. After the first bubbling period a spectrum of the hydride region was accumulated with 512 scans under a hydrogen pressure of 3 bar. The spectrum (Figure S6) in thermal equilibrium of the hydride region of this solution shows only a small hydride signal arround -22 ppm. This signal is attributed to a stable side product, resulting from the onset of degradation of the catalytic active rhodium species.

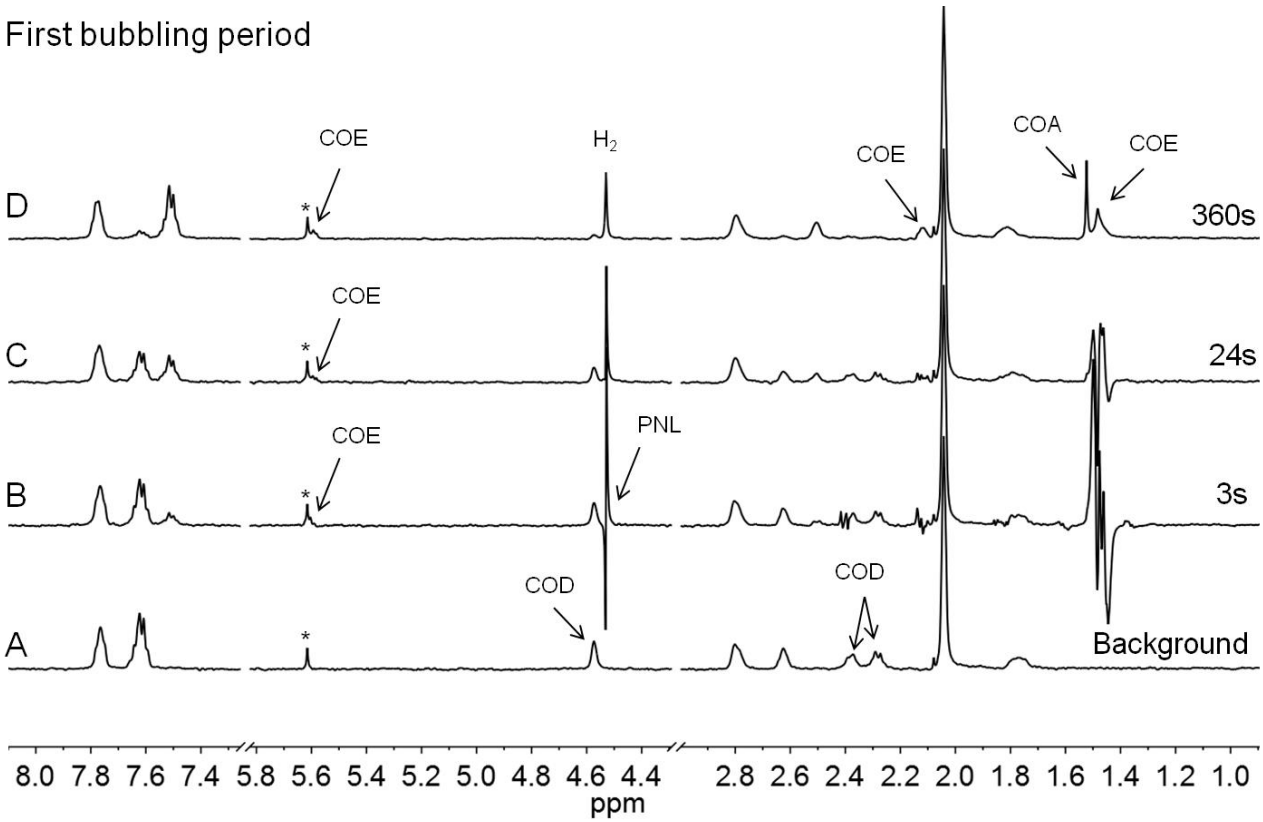

Figure S5. ^{1}H 500 MHz NMR spectra series of a catalyst solution (4.5 mM) in acetone-d_6, recorded with 5 degree detection pulse. Spectrum A) is taken before first bubbling by parahydrogen, B) 3 s, C) 24 s and D) 360 s after first bubbling with parahydrogen (3 bar). The spectra show the activation of the catalyst (hydrogenation of COD to COE and further to COA) and the PNL at 4.55 ppm. The asterisk marks an impurity.

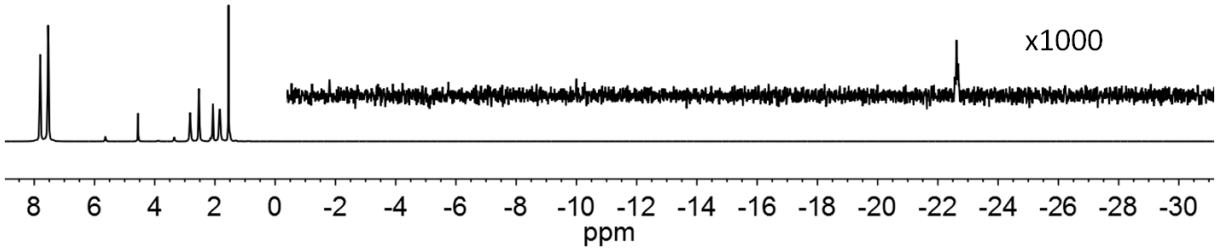

Figure S6. Thermal ^{1}H NMR spectrum of a catalyst solution (4.5 mM) in acetone-d_6; accumulated 360s after first bubbling by parahydrogen. The spectrum has 512 scans measured at 500 MHz during 30 minutes. The insert display the dihydrogen and dihydride region, magnified by factor of 1000.

Before the second bubbling period was started a background spectrum of the solution was recorded. This spectrum A (Figure S7) shows that the COE in the solution is completely hydrogenated to COA. In spectrum B, recorded 3s after the parahydrogen injection was stopped, a strong PNL at 4.55 ppm is clearly visible. The signal of the PNL line decays rapidly and after 24 s the the PNL is no longer observable. The accumulated spectrum of the hydride region recorded 360 s after parahydrogen injection shows an increasing number of very tiny hydride species signals. These signals show clearly the degradation of the catalyst due to further hydrogen treatment.

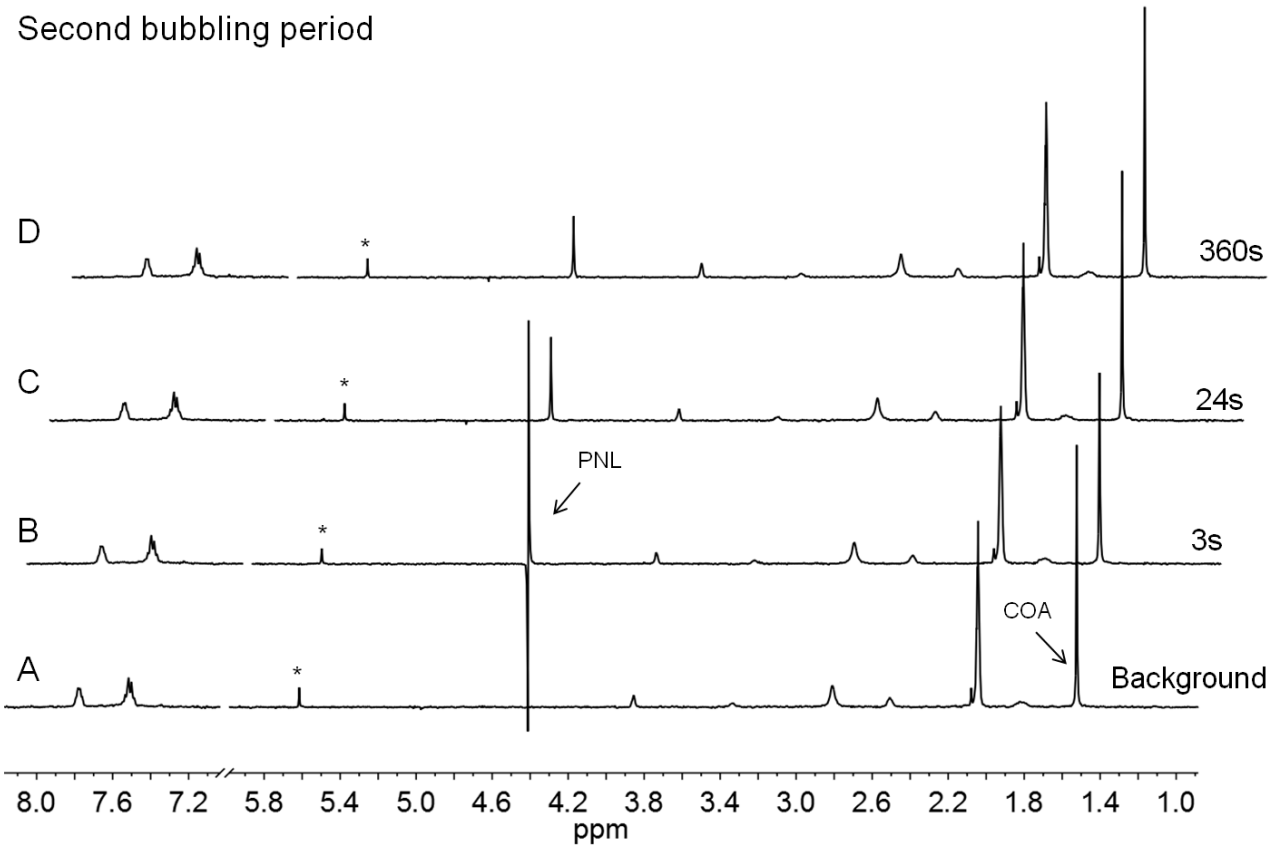

Figure S7. ^{1}H 500 MHz NMR spectra series of a catalyst solution (4.5 mM) in acetone-d_6, A) taken before second bubbling by parahydrogen, B) 3 s, C) 24 s and D) 360 s after second bubbling with parahydrogen (3 bar). The spectra show a completely activated catalyst (all COD is hydrogenated to COA) in the beginning and the PNL at 4.55 ppm. The asterisk marks an impurity.

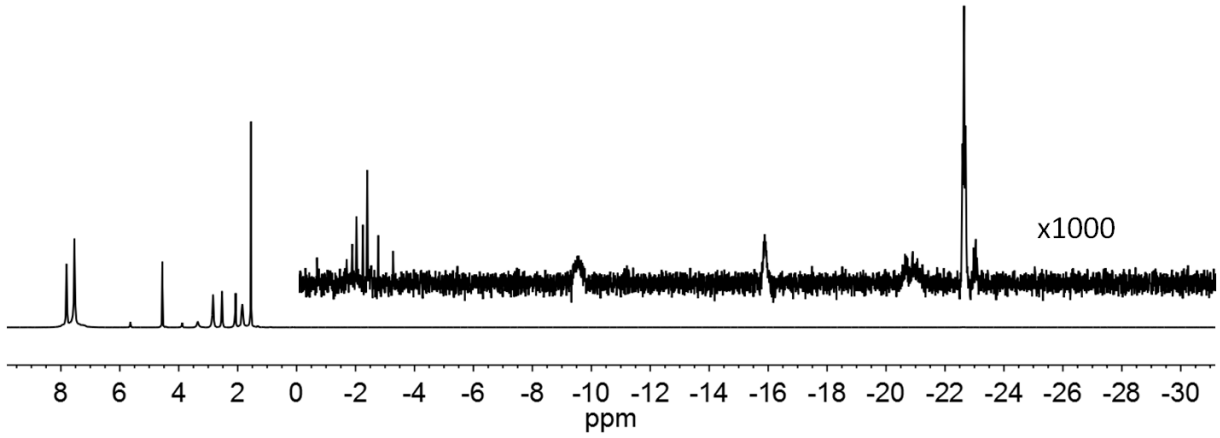

Figure S8. Thermal ^{1}H NMR spectrum of a catalyst solution (4.5 mM) in acetone-d_6; accumulated 360s after second bubbling by parahydrogen. The spectrum has 512 scans measured at 500 MHz during 30 minutes. The insert display the dihydrogen and dihydride region, magnified by factor of 1000.

The process of catalytic degradation is more clear in the third spectra series recorded during the third bubbling period of parahydrogen (Figure S9). Even the background spectrum A show additional

signals and decreased signals of the phenyl groups at the aromatic region. Moreover after the injection of parahydrogen no PNL occurs. Which indicates a complete degradation of the active species which is responsible for the para-ortho conversion. In the accumulated spectrum of the hydride region a bigger number of hydride signals are seen (Figure S10).

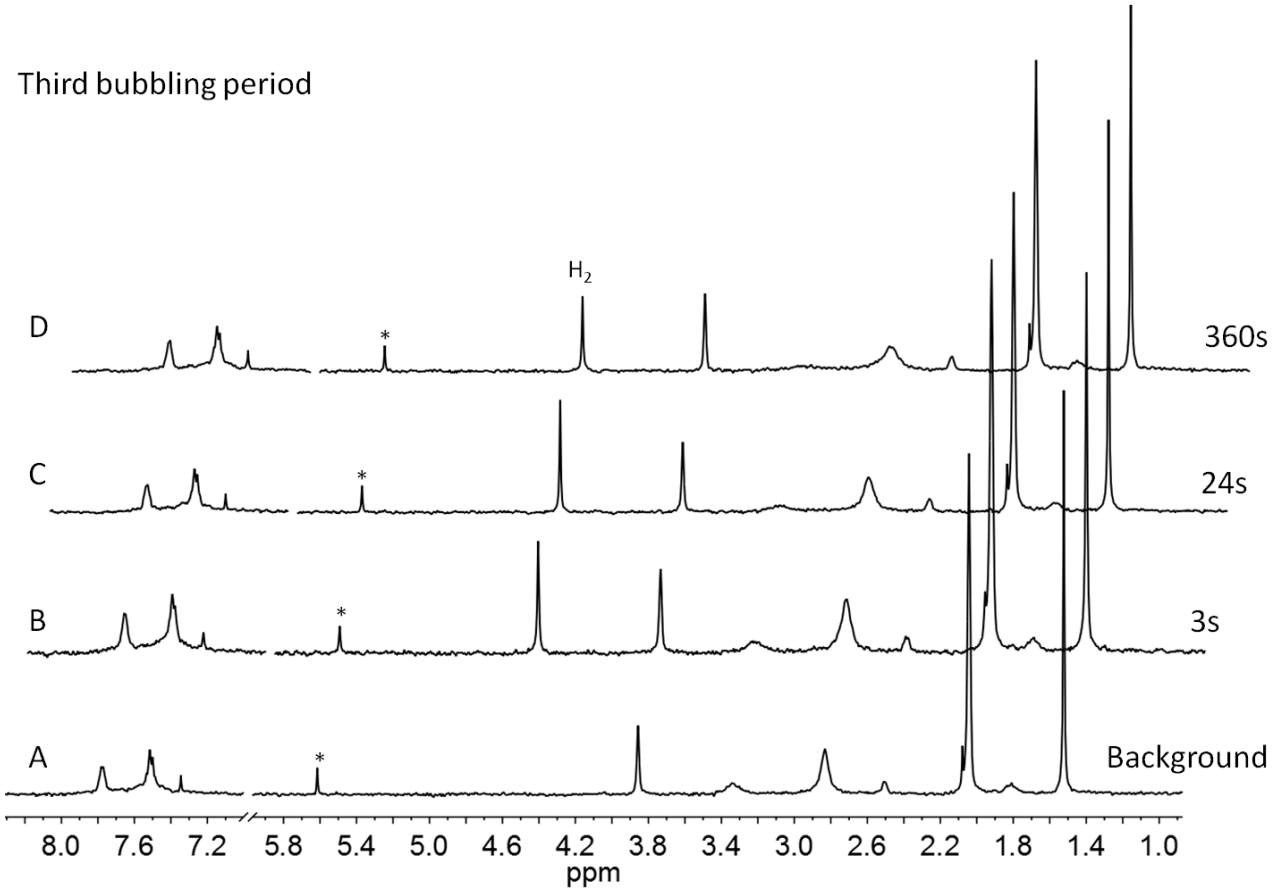

Figure S9. ^{1}H 500 MHz NMR spectra series of a catalyst solution (4.5 mM) in acetone-d_6. A) taken before the third bubbling by parahydrogen, B) 3s, C) 24s and D) 360s after third bubbling with parahydrogen (3bar). The spectra series shows the degradation of the catalyst due to further treatment with hydrogen. No PNL is observable. The asterisk marks an impurity.

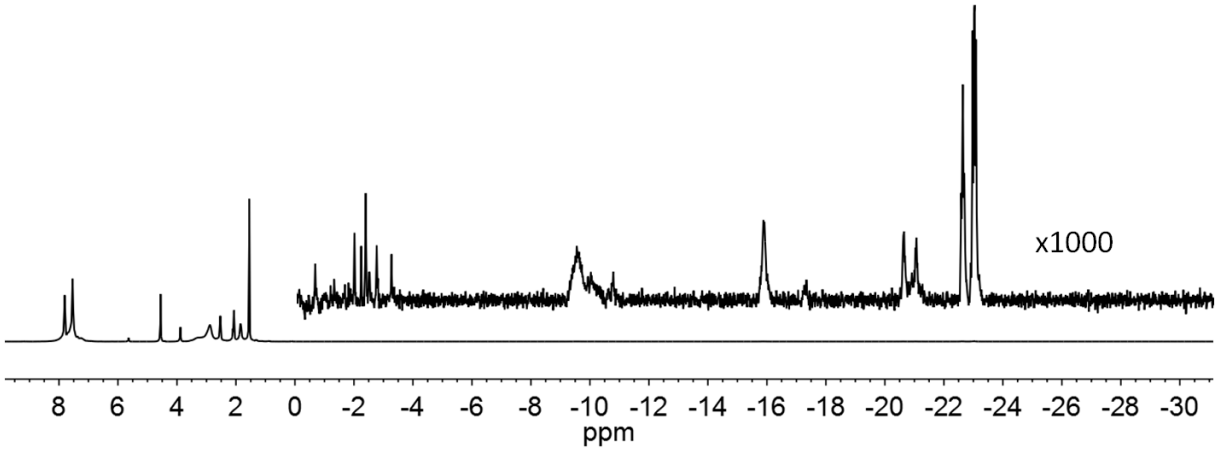

Figure S10. Thermal ^{1}H NMR spectrum of a catalyst solution (4.5 mM) in acetone-d_6; accumulated 360s after third bubbling by parahydrogen. The spectrum has 512 scans measured at 500 MHz during 30 minutes. The insert display the dihydrogen and dihydride region, magnified by factor of 1000. Due to the degradation of the catalyst more hydride signals appear in the spectrum.

Kinetics of the PNL signal

As has been mentioned previously, the PNL is only present after the bubbling with of *p*-H_2 and decays rapidly in time. Figure S11 (a) displays a kinetic experiment, where after the initial bubbling (30 s) of the *p*-H_2 a series of FIDs with small flip-angle (5°) pulses were recorded. The delay time between the pulses was 3.5 s; bubbling pressure was 3 bar; 1.8 mM of catalyst in acetone. The PNL decays rapidly with decay time about 4.5 s (Figure S11 (b)).

Employing an external reference sample of 50.0 mM of Acetyl-Alanine in methanol-d_4, measured under equivalent conditions, the absolute intensities of the PNL were converted into concentrations to allow a direct comparison of the PNL signal relative to the proton signal of NMR solvents. It is found that the initial intensities of the PNL, shortly after the bubbling, are rather high (100-150 mM in units of concentration). These values are comparable to the residual solvent signal of protons in commercial deuterated solvents: 99.5% acetone-d_6 (70mM residual protons), 99.5% methanol-d_4 (130 mM residual protons).

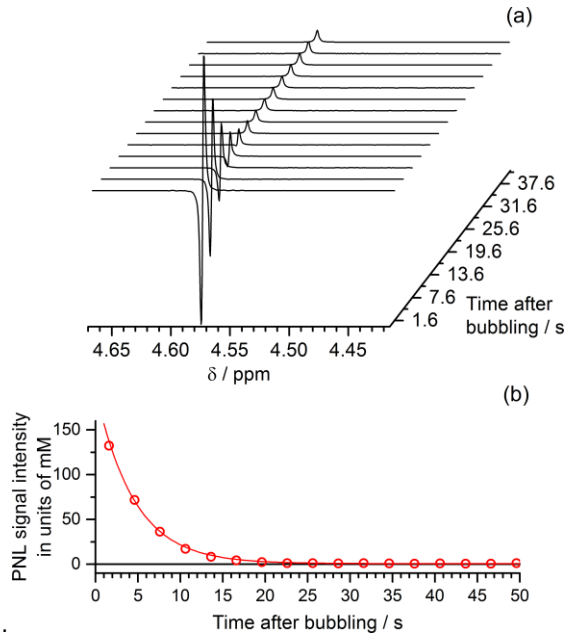

Figure S11. (a) ^{1}H NMR spectra of the H_2 region from 4.67-4.42 ppm, detected by a 5° flip angle after bubbling a catalyst solution (1.8 mM in acetone-d_6) by p-H_2. (b) Kinetics of PNL line intensity. An external reference sample of 50.0 mM of Acetyl-Alanine in methanol-d_4, measured under the same conditions, was employed to convert the NMR signal intensities into concentrations. Experimental data points were fitted by exponential function: $y=y_0+A*\exp(-t/\tau)$. The best fit was found at τ=4.5 s.

Failure to direct detection of intermediate complex with parahydrogen

In principle it could be possible to directly detect the hydride intermediates by a PASADENA experiment. Figure S12 displays a PASADENA experiment of the catalyst solution in acetone-d_6 after bubbling by p-H_2. There are no visible signals in the range of -15 ppm. Thus at our experimental conditions resonance lines of intermediate complex are beyond the limit of direct detection.

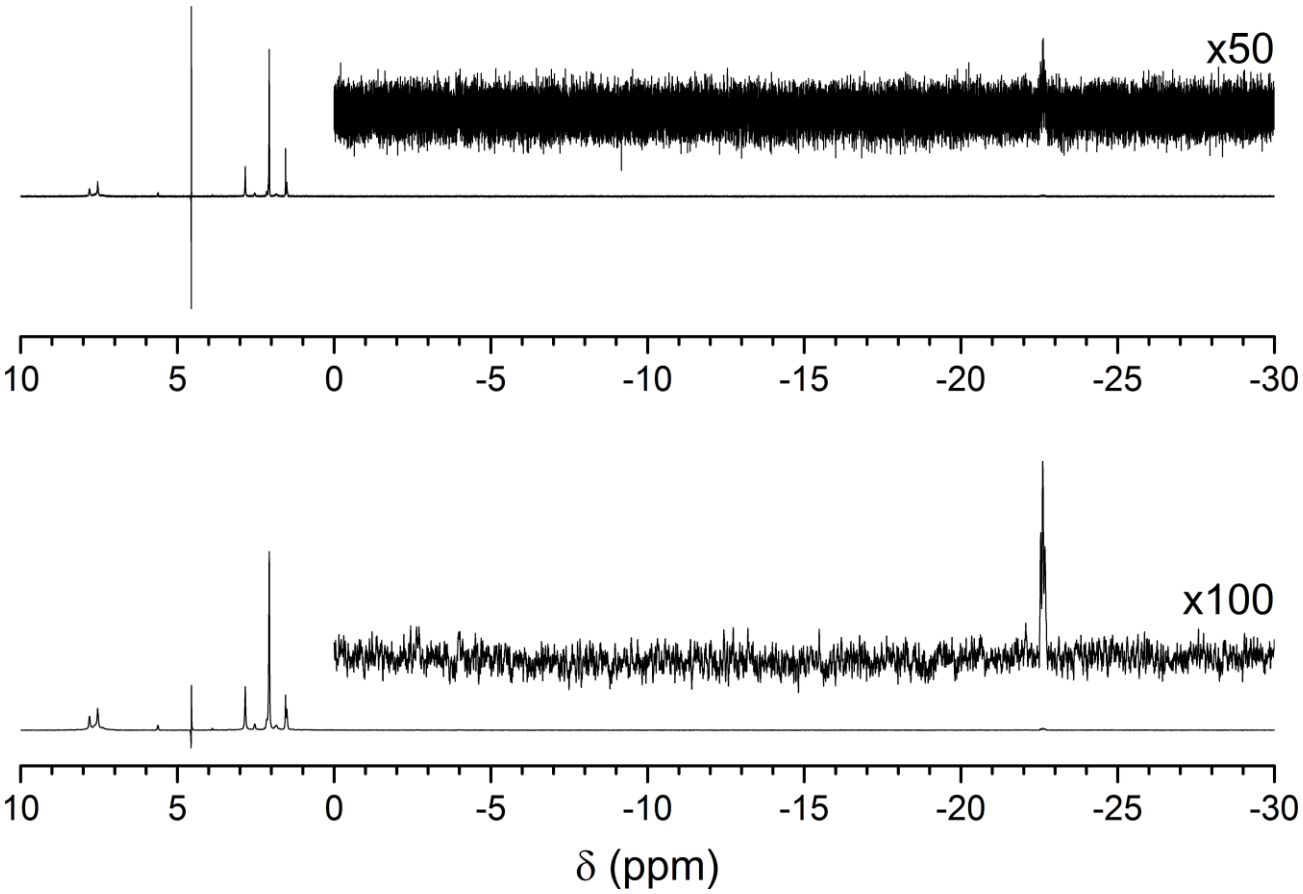

Figure S12. PASADENA ^{1}H-NMR spectrum detected after bubbling by parahydrogen (50%) at 2 bar. Solution of catalyst (3.8 mM) in acetone-d_6, bubbling period 60 s, delay after bubbling 2.2 s, detection pulse $\pi/4$. Spectrum processed with the line broadening 0.1 Hz (upper spectrum) and 5 Hz (lower spectrum). Inserts show magnified view of the region from -10 to -30 ppm.

PANEL experiment – comparing n-H_2 and p-H_2

Figure S13 compares the PANEL spectra using p-H_2 and 45° detection with the equivalent experiment using n-H_2 and 90° detection as a function of the frequency υ_{CW}. While the spectrum obtained with p-H_2 clearly reveals the signals in the hydride region, the spectrum obtained with n-H_2 displays only the signal of the dissolved hydrogen at 4.5 ppm.

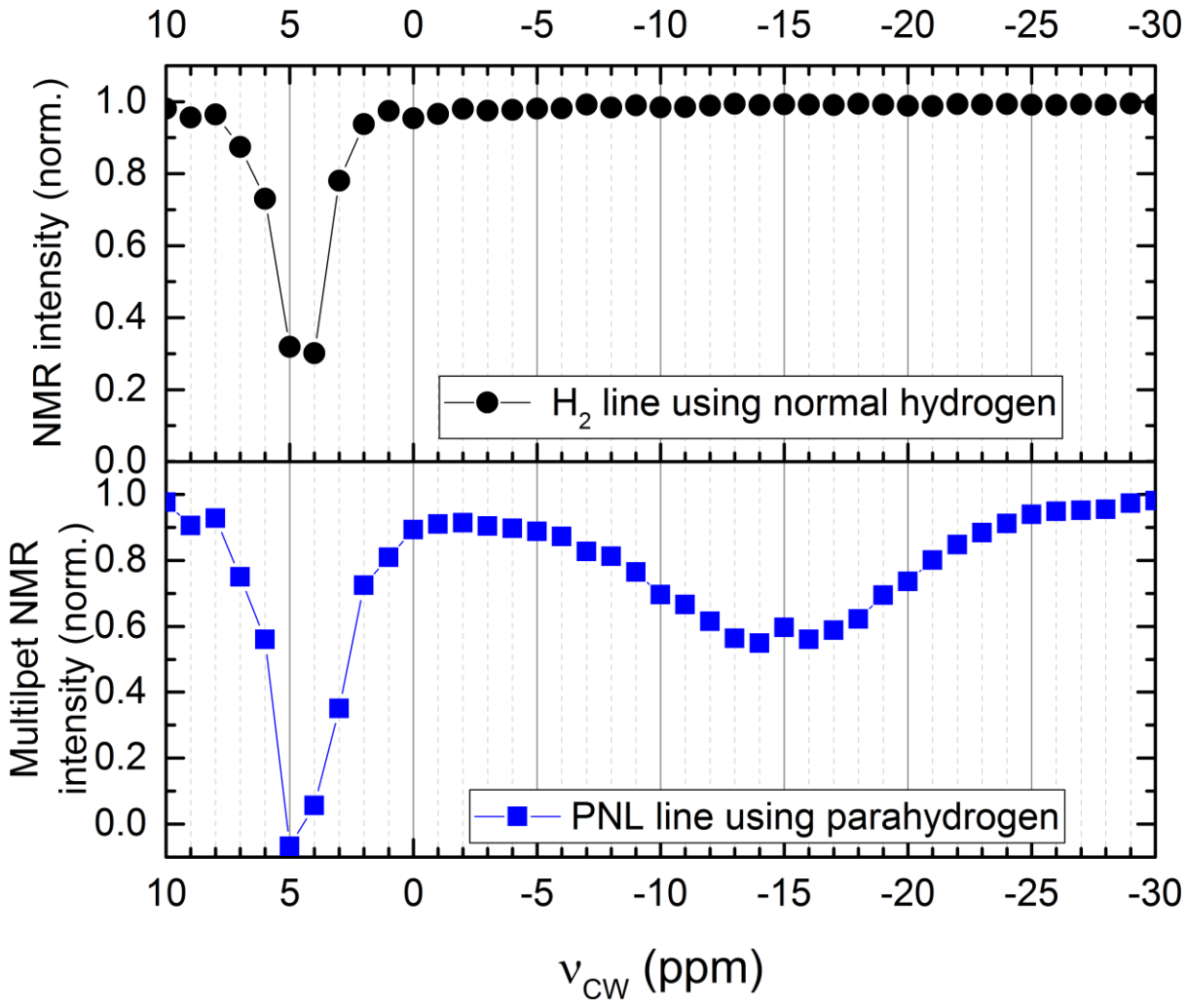

Figure S13. PANEL experiments employing n-H2 (upper panel) and p-H2 (lower panel). Duration of bubbling 4 s, RF irradiation time 2 s, bubbling pressure 2 bar, concentration of catalyst in acetone-d_6 2.4 mM. ($\upsilon_1 = 0.5$ kHz)

Solvent Dependence of the PNL Signal

Figure S14 and Table S1 compare the phase and intensity of the PNL for different solvents. While in all solvents where the catalyst is soluble, a PNL is found with the same phase there is no PNL in the solvents where the catalyst is insoluble.

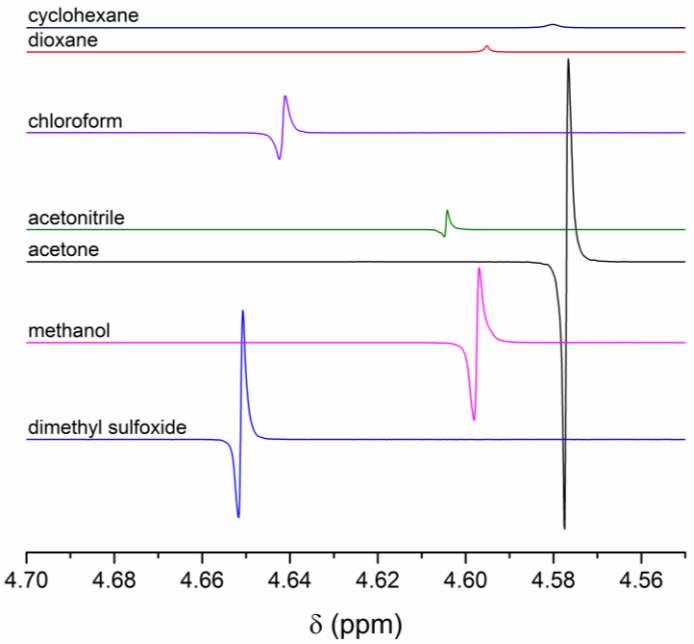

Figure S14. Spectra of PNL in different solvent. Detection NMR pulse is π/4. Experimental conditions: 1 mg of catalyst in 0.7 ml of solvent (2 mM), bubbling pressure 2 bar, bubbling duration 20 s, delay between bubbling and detection 2s, detection flip angle π/4, resonance frequency 700 MHz.

Table S1. Summarized results for the appearance of the PNL in different solvents.

Solvent	Solubility of catalyst	PNL line	Phase of PNL detected by π/4 flip angle
Aceton-d_6	good	yes	emission-absorption
Dioxane-d_8	insoluble	no	no PNL signal
DMSO-d_6	good	yes	emission-absorption
Methanol-d_4	good	yes	emission-absorption
Acetonitril-d_3	good	yes	emission-absorption
Cyclohexane-d_{12}	insoluble	no	no PNL signal
CDCl3	good	yes	emission-absorption

Pulse program for the PANEL experiment

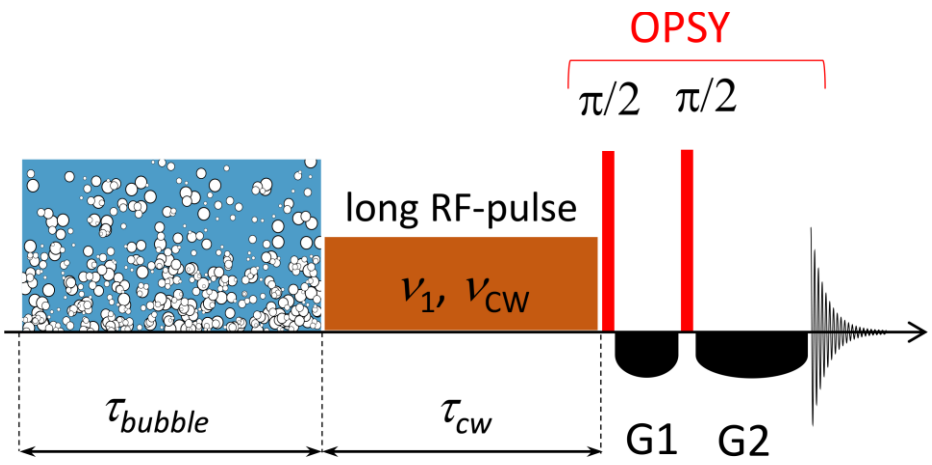

Figure S15. The PANEL (PArtially NEgative Line) experiment for the indirect detection of the hydrogen catalyst complex.

NMR pulse program for the PANEL (PArtially NEgative Line) experiment for Bruker Avance III spectrometers running TopSpin 3.2 software equipped with a computer controlled *p*-H_2 and N_2 source:

Main code is written in black, all comments are colored in green

```
#include <Avance.incl> ;standard include file
#include <TTLvalves.incl> ; include file which contains description of short
;commands for opening and closing TTL-magnetic valves
#include <Grad.incl> ;standard include file
; commands for operating magnetic valves
; IN_ON, IN_OFF, pH2_ON, pH2_OFF, Ar_ON, Ar_OFF,
; OUT_ON, OUT_OFF, VAC_ON, VAC_OFF, E_ON, E_OFF, REG_ON, REG_OFF
; IN=input to the NMR sample tube
; OUT=output from the NMR sample tube
; pH2=parahydrogen source
; Ar=inert gas source
; VAC=vacuum source
; E= valve to equilibrate input and output pressure
; REG=final backpressure regulator

"acqt0=-p1*2/3.1416"

define list<frequency> fqlist=<$FQ1LIST> ; definition of frequency list for
;scanning CW frequency

1 ze
10u pl9:f2
;clean pipes
500m VAC_ON
100m VAC_OFF


100m LOCKH_ON ;block LOCK
200m pH2_ON
```

```
1s IN_ON OUT_ON REG_ON ; START p-H2 pre-bubbling (to fill line with pH2)
      50m pH2_OFF
      50m E_ON ; STOP pre-bubbling

2 ze

 10u fqlist:f2
 20u fqlist.inc ; increment frequency list

50m E_OFF
d3 pH2_ON ; START p-H2 bubbling with duration d3
50m pH2_OFF
50m E_ON ; STOP p-H2 bubbling

d2 cw:f2  ;CW irradiation with duration d2, power pl9, frequency from FQ1LIST
20u do:f2 ; stop CW irradiation

;OPSY block start (OPSY block can be replaced by simple 45-degree pulse)
  p1 ph1
  d12 gron1
  250u groff
  p1 ph1
  d13 gron2
  250u groff
;OPSY block end
  go=2 ph31
  50m wr #0 if #0

  lo to 2 times td1

50m IN_OFF E_OFF REG_OFF OUT_OFF
100m LOCKH_OFF ;unblock LOCK

exit

ph1=0
ph31=0


;pl1 : f1 channel - power level for OPSY pulses
;pl1 : f2 channel - power level for CW irradiation
;p1 : f1 channel -  90 degree high power pulse
;d3 : p-H2 bubbling time
;d2 : CW irradiation time
;td1: number of experiments equal to the number of items in frequency list
```

Literature

1. Geen, H.; Freeman, R., Band-Selective Radiofrequency Pulses. *J. Magn. Reson.* **1991**, *93*, 93-141.

2. Aguilar, J. A.; Elliott, P. I. P.; López-Serrano, J.; Adams, R. W.; Duckett, S. B., Only Para-Hydrogen Spectroscopy (OPSY), a Technique for the Selective Observation of Para-Hydrogen Enhanced NMR Signals. *Chem. Commun.* **2007**, 1183-1185.